29-14

Effects of hydrothermal circulation on temperatures in rupture zone of the great 1960 Chilean earthquake

Holly M. M. Rotman (hrotman@nmt.edu) and Glenn A. Spinelli
Earth & Environmental Sciences, New Mexico Institute of Mining and Technology, Socorro, NM

IA. Objectives

1. Estimate subduction fault temperatures in the south Chile subduction zone;
2. Examine effects of fluid circulation in ocean crust on subduction fault zone temperatures;
3. Find a preferred thermal state of the Chile megathrust in the 1960 rupture patch.

IB. Why Model Fault Zone Temperatures?

Stick-slip behavior of granite suggests temperature dependence (Figure 1).

Starting at ~150°C, a number of diagenetic reactions affect the mechanical behavior of material along a subduction zone plate interface: opal ➔ quartz; smectite ➔ illite; carbonate precipitation.

As temperatures approach 350°C, rocks begin to behave ductilely rather than brittlely, and thus no longer store sufffficient stress to produce a (large) earthquake.

So, identifying this temperature range is helpful to estimating the megathrust rupture zone.

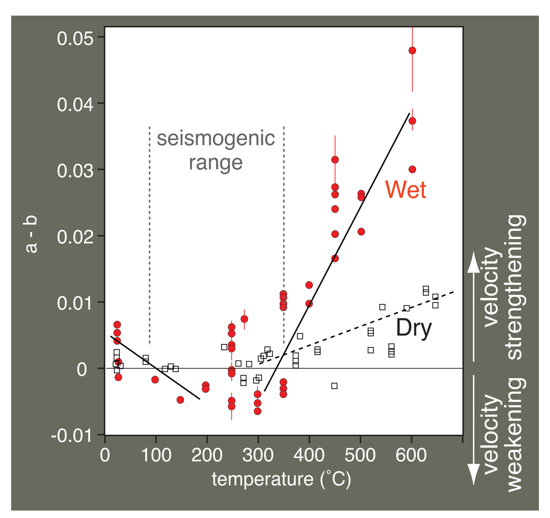

Figure 1. Results of laboratory experiments on wet and dry granite samples. a-b represents the change in friction upon increasing sliding velocity. If negative, it indicates velocity-weakening behavior, where initiated slip is likely to continue and result in an earthquake. If positive, it indicates velocity strengthening, where friction increases and slip ceases. The 'seismogenic range' falls in the temperatures of velocity weakening behavior. Modified from Blanpied et al., 1995.

IC. Why Include Fluid Flow?

At Nankai (Japan), basic thermal models did not match the observed surface heat flux near the trench (Figure 2).

However, a model including thermal effects of fluid circulation in the ocean crust more effectively matched heat flux data.

The uppermost layer of the subducting slab contains an aquifer, in which vigorous fluid circulation acts to exchange heat, cooling subducted crust and warming crust near the trench.

The Nankai example is most dramatic, due to a relatively thin sediment layer; thick sediment suppresses high heat flux at the trench.

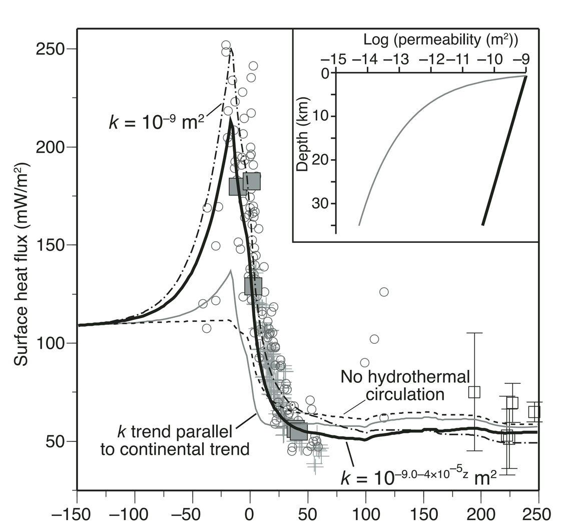

Figure 2. Measured heat flux and models at the Nankai margin. Flux measurements are from land boreholes, ODP drill sites, gas hydrates (BSR), and probes. Note the conductive model (dashed) does not fit data seaward of trench. However, models with fluid flow effects from a high-permeability aquifer demonstrates the spike in heat flux at the trench. From Spinelli and Wang, 2008.

II. Location

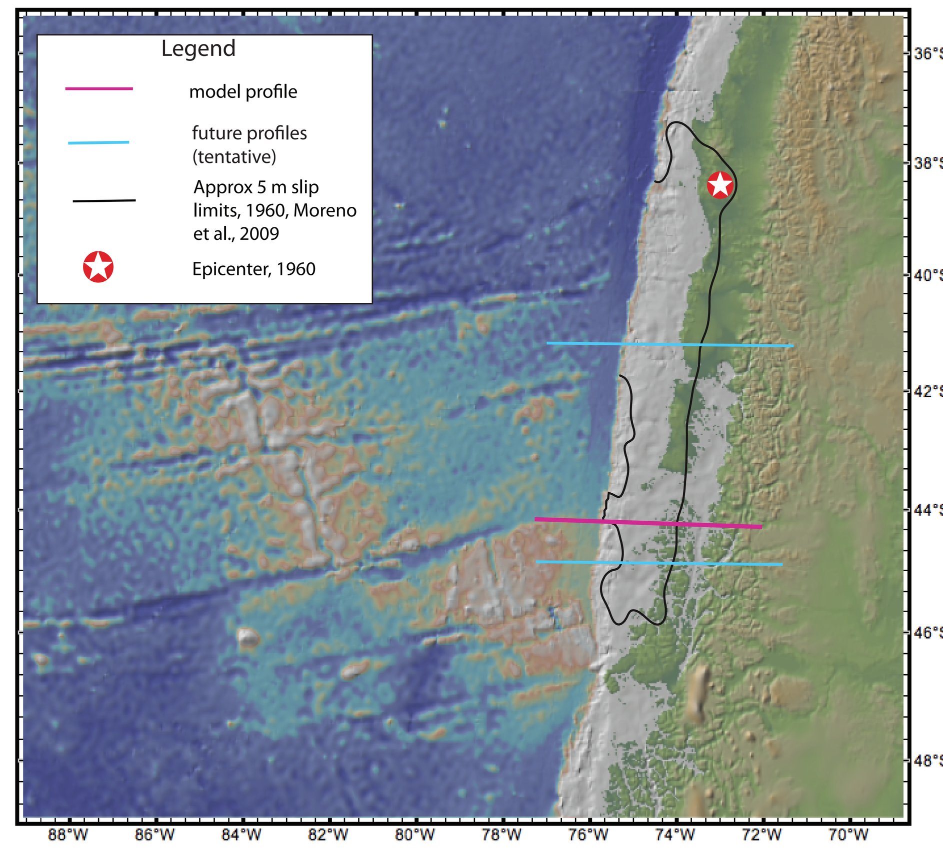

Figure 3. Location of 1960 slip and modeled profile. At the trench, there is ~1 km of sediment and the ocean crust is ~15 m.y. old. Basemap taken in GeoMapApp. 1960 epicenter and slip from Moreno et al., 2009.

III. Plan of Attack

1. Construct steady-state finite element model
   - -Profile -150 to +400 km from trench
   - -Physical properties (e.g., conductivity, radiogenic heating, slab dip, convergence velocity, slab age)
2. "Final" output: surface heat flux, megathrust temperatures:

2a. Generate model for conductive situation first

2b. Generate models for range of permeabilities for fluid flow case

3. Estimate temperatures on fault zone in seismogenic range

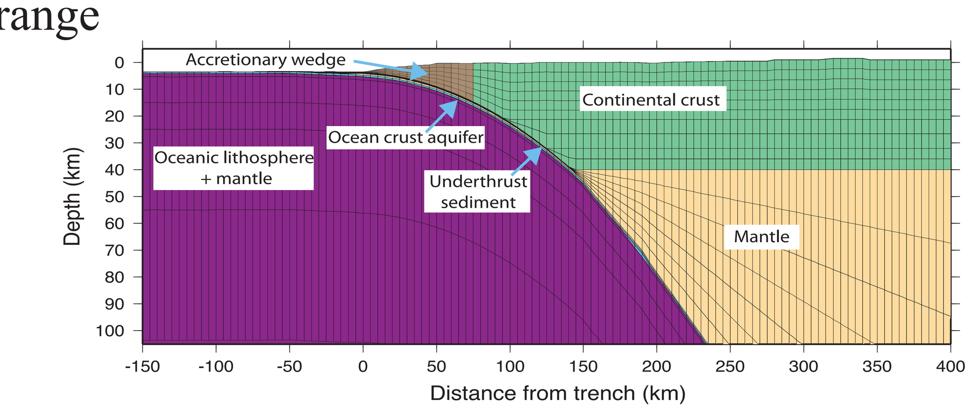

Figure 4. Model grid. Physical properties are changed gradually landward in the wedge to the continental crust.

IV. Preliminary Results

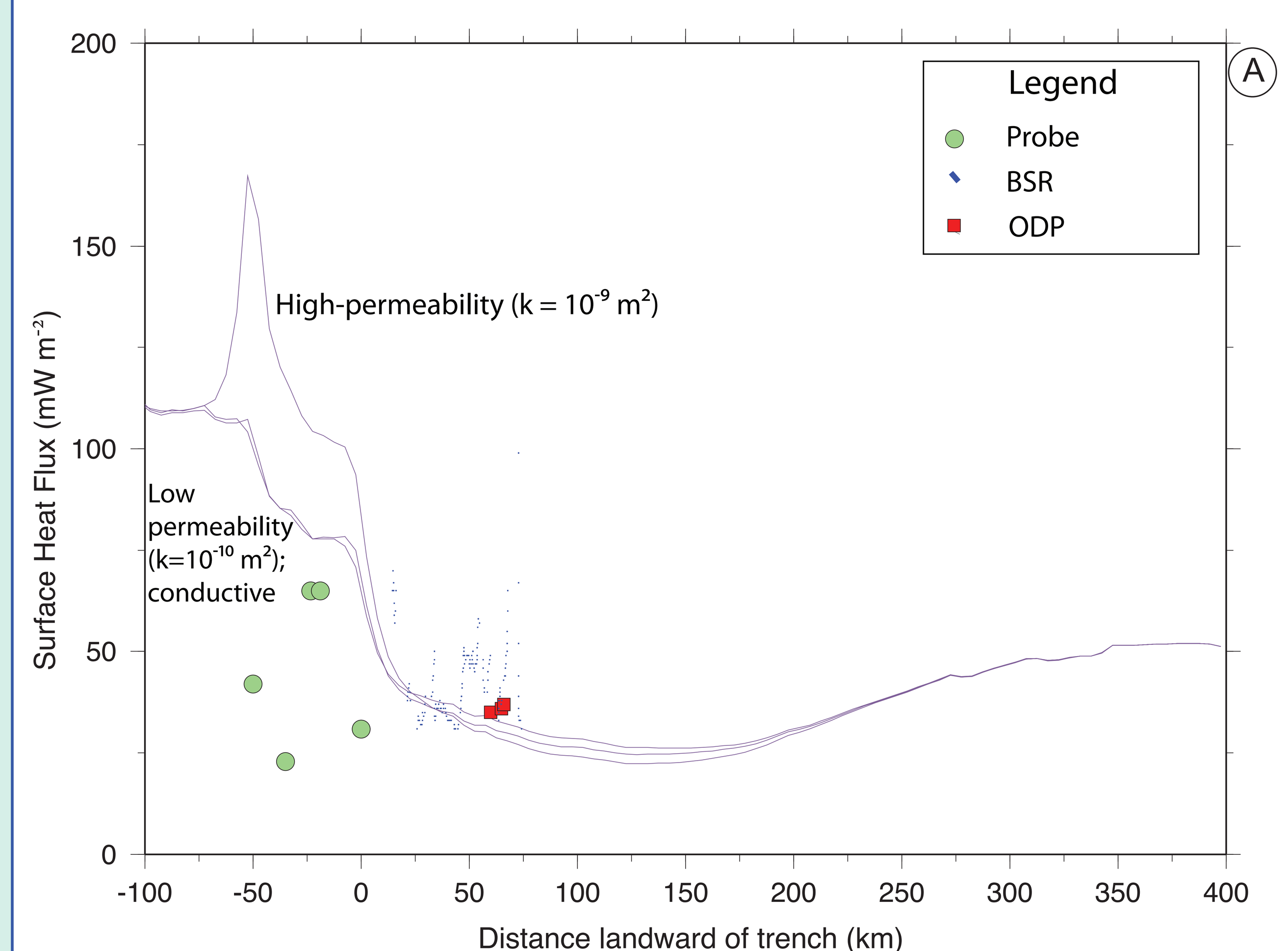

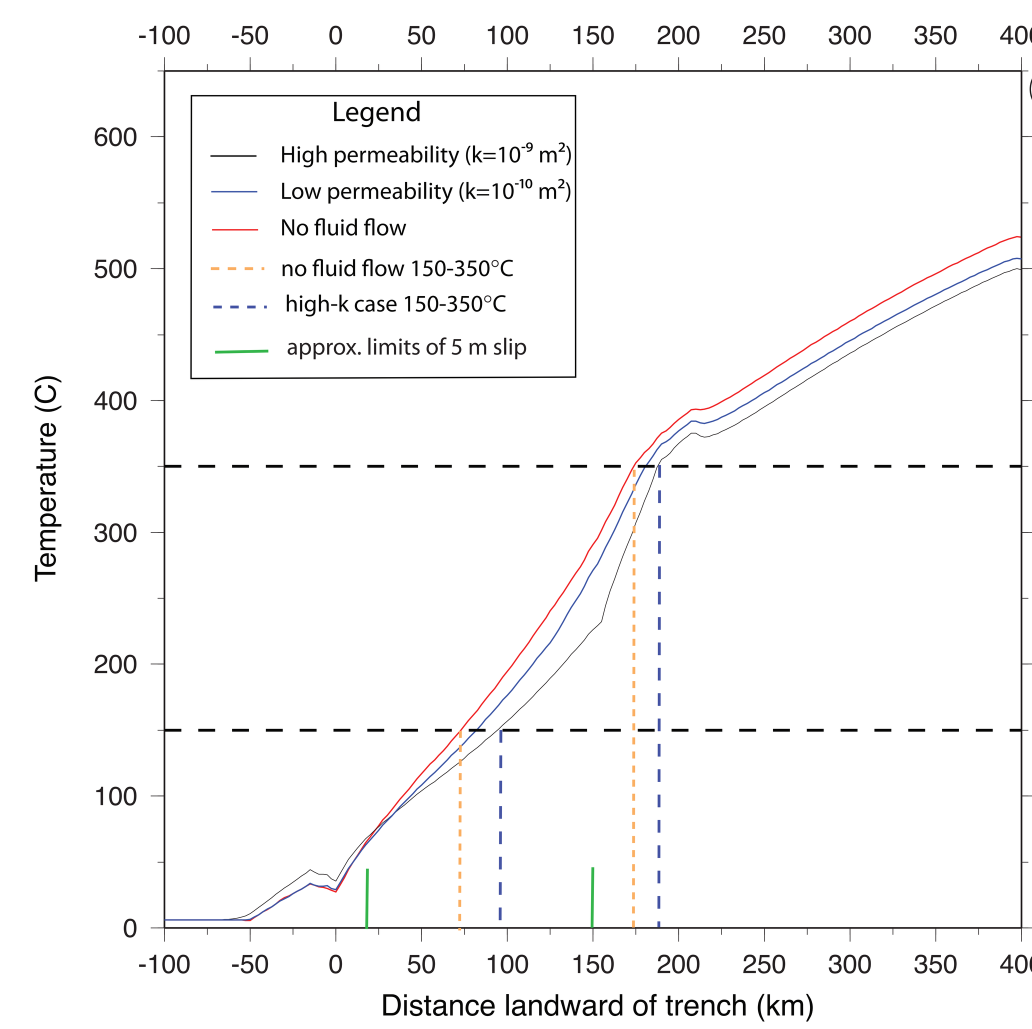

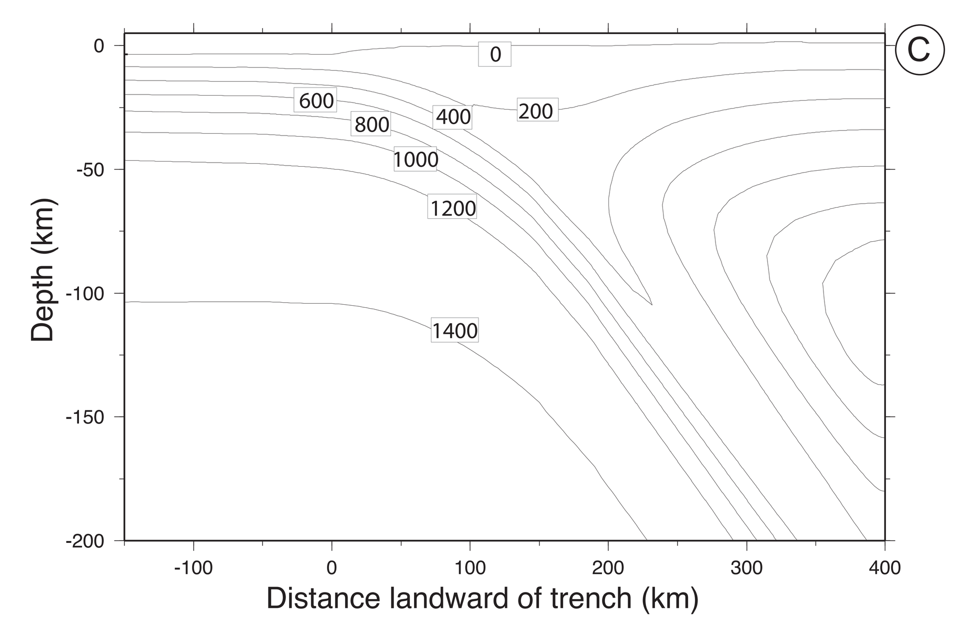

Figure 5. A) Modeled heat flux against distance from trench, Chile, 44°S. Data from Ocean Drilling Program (ODP) boreholes are the most robust measurements. Low permeability (10^{-10} m^2) case is almost identical here to the conductive (no fluid flow) case. B) Megathrust temperatures against distance landward of the trench. Approximate limits of 5 m slip are from Moreno et al. (2009) in Figure 3. The seismogenic temperature range from Figure 1 is marked (150 - 350°C). In the conductive case, 150 - 350°C is 75 - 175 km from the trench. In the high permeability case, 150 - 350°C is 100 - 190 km from the trench. Note the 5 m limits are seaward of these. C) Contour plot of temperatures, every 200°C. Downdip extension of the 400°C isotherm is due to the relatively cold downgoing Nazca slab.

V. Discussion

-Including ocean crust fluid circulation shifts 150° and 350°C downdip, as expected for an aquifer drawing heat from downdip up to the trench.

-Model results yield temperatures in the >5 m slip zone (Figure 6) of ~70°C (updip) to ~250°C (downdip).

-Surface heat flux data (Figure 5A) near the trench offers no constraints for discriminating between models with or without fluid circulation in the ocean crust; more, high-quality heat flux observations on the incoming plate are necessary to provide thermal constraints.

-350°C is reached ~60-70 km depth, ~20 km below the continental Moho, consistent with existing conductive models of the Chilean subduction zone.

-Therefore, the downdip limit of the seismogenic zone may be controlled by the Moho intersection rather than temperature.

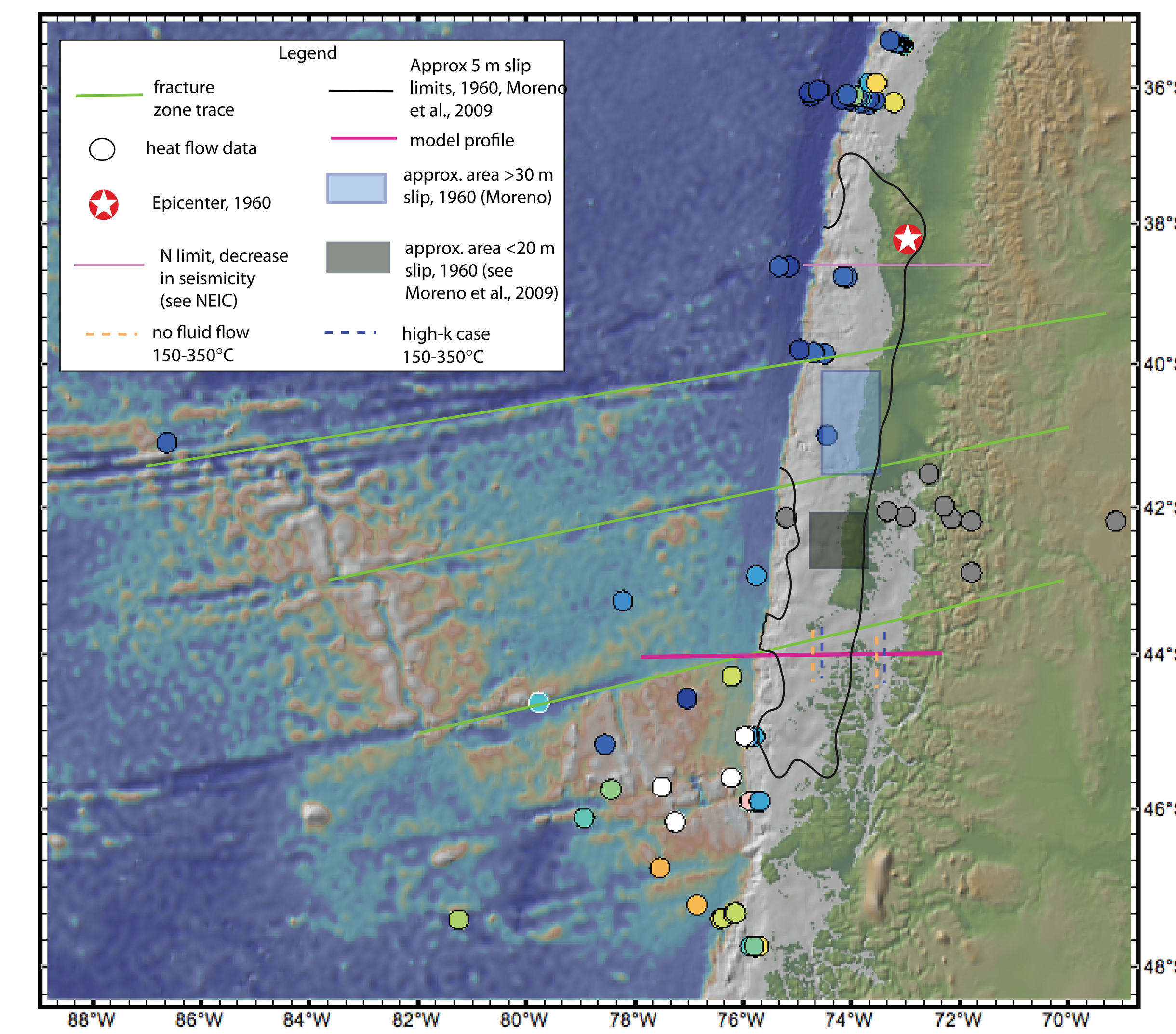

Figure 6. Figure 3 updated to show results and other potentially relevant information. There is a ~8 m.y. age jump across the fracture zone in the 44°S profile. Heat flux data seaward of the trench, helpful in model constraints, are sparse with distance from the Chile Triple Junction at ~46°S.

VI. Future Work

1. Thermal model profiles at ~45°S and ~41°S or ~39°S.
2. Comparison of results with: surface heat flux data, 1960 slip models, coseismic deformation data, conductive thermal models, basalt-eclogite transition* of Nazca slab, and slow slip* events in south Chile. (*if available)
3. Possible thermal models in the rupture zone of the 2010 M8.8 Maule earthquake.
4. This work is being conducted as part of a NSF-funded (award EAR-0943994 to Spinelli) doctoral project on subduction zone earthquakes. I will also be completing thermal models in other subduction zones (e.g., Alaska, Sumatra).

Key References

Blanpied, M.L., Lockner, D.A., and Byerlee, J.D., 1995, Frictional slip of granite at hydrothermal conditions, Journal of Geophysical Research, v. 100, p. 13045-13054.

Haberland, C., Rietbrock, A., Lange, D., Bataille, K., and Dahm, T., 2009, Structure of the seismogenic zone of the southcentral Chilean margin revealed by local earthquake traveltime tomography, Journal of Geophysical Research, v. 114, doi:10.1029/2008JB005802

Moreno, M.S., Bolte, J., Klotz, J., and Melnick, D., 2009, Impact of megathrust geometry on inversion of coseismic slip from geodetic data: application to the 1960 Chile earthquake, Geophysical Research Letters, v. 36, doi:10.1029/2009/GL039276

Oleskevich, D.A., Hyndman, R.D., and Wang, K., 1999, The updip and downdip limits to great subduction earthquakes: thermal and structural models of Cascadia, south Alaska, SW Japan, and Chile, Journal of Geophysical Research, v. 104, p. 14965-14991.

Spinelli, G.A., and Wang, K., 2008, Effects of fluid circulation in subducting crust on Nankai margin seismogenic zone temperatures, Geology, v. 36, p. 887-890.